ChemComm

Accepted Manuscript

This article can be cited before page numbers have been issued, to do this please use: X. Han, C. Huang, X. Chen, Y. Lu and W. Yang, *Chem. Commun.*, 2015, DOI: 10.1039/C5CC05229G.

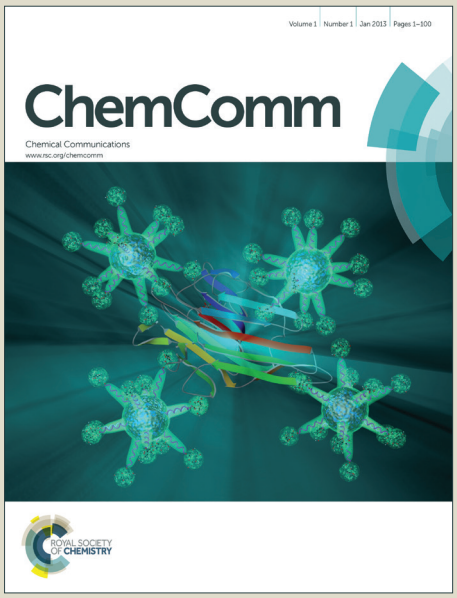

ROYAL SOCIETY OF CHEMISTRY

www.rsc.org/chemcomm

View Article Online
DOI: 10.1039/C5CC05229G

ChemComm

RSCPublishing

COMMUNICATION

Anodic electrogenerated chemiluminescence of self-assembled peptide nanotubes in aqueous system

Cite this: DOI: 10.1039/xOxx00000x

Xue Han,[a] Chunxiu Huang,[a] Xu Chen,*[a] Yanluo Lu [a] and Wensheng Yang*[a]

Received 00th January 2012,
Accepted 00th January 2012

DOI: 10.1039/xOxx00000x

www.rsc.org/

Anodic electrogenerated chemiluminescence (ECL) of the self-assembled peptide nanotubes (PNTs) modified electrode in aqueous system was observed for the first time using tri-*n*-propylamine (TPrA) as the coreactant. The potential application of ECL PNTs in analytical chemistry was also demonstrated using Cu^{2+} as an example.

Bioinspired nanomaterials, especially derived from peptide building blocks, have attracted increasing interest because of their biocompatibility, functional flexibility and molecular recognition capability.[1] Among various peptide-based building blocks, diphenylalanine (FF, Fig.1A) is the simplest biological molecule, which was found in the key motif of Alzheimer's β-amyloid.[2] The FF dipeptide and its analogues can self-assemble into various nanostructures, such as nanotubes (PNTs), nanowires, nanospheres and organo/hydrogels. These nanostructures exhibit novel physical and chemical properties, which make them potential applications in some fields including energy storage devices, drug delivery agents, piezoelectric components and biosensing.[3] Recently, the photoluminescence (PL) of the self-assembled PNTs has been reported and studied in detail.[4] Interestingly, quantum confinement (QC) phenomenon that was found usually in semiconductor crystals, has been observed in the PNTs,[4a] as well as peptide nanospheres[5a] and hydrogels.[5b] Further investigation indicated that the occurrence of QC in these structures was due to a crystalline structure of subnanometer scale dimension (also called as biological quantum dots) formed under the self-assembly process.[4b] The synergistic effect of millions of quantum dots (QDs) in a single nanotube could lead to exceptional electronic and photonic properties of the PNTs, which make them a new and environmentally clean candidates for luminescence devices.[6]

Electrogenerated chemiluminescence (ECL) has been proven to be a powerful detection technique.[7] Compared with chemiluminescence and fluorescence, ECL has many advantages, such as its easy controllability, low background and higher sensitivity. In recent years, the application of ECL in biological analysis has been rapidly expanded. Various new ECL emitters such as silicon nanocrystals,[8a] carbon QDs[8b] and Au nanoclusters[8c] as well as organic luminophores[8d,e] have been developed successively. However, the ECL emission efficiency of these inorganic nanoemitters[8a-c] is lower. Although organic ECL emitters[8d,e] have much higher emission efficiency than inorganic emitters, the stable ECL emission in aqueous system was difficultly obtained based on these organic ECL emitters so far. This largely limits the application of organic ECL luminophores in biological analysis. Therefore, the development of new, highly efficient, nontoxic and tunable ECL emitters are still highly desirable.[9]

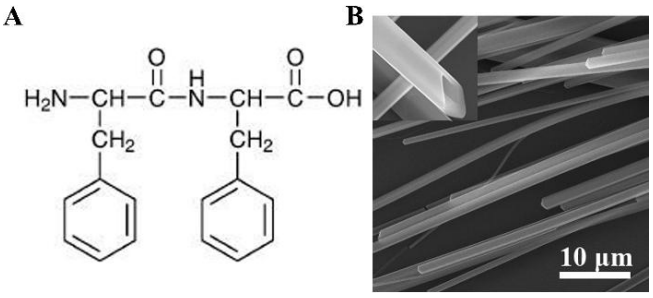

Fig. 1 (A) Molecular structure of FF. (B) A typical SEM image of PNTs. The inset displays the enlarged view

Owing to the notable PL and QC properties,[4,5] FF-based self-assembled nanostructures as a new kind of biological semiconductors have potential as ECL emitters. Nevertheless, reports on the ECL behavior of peptide nanostructures are very rare. Only our group previously reported the cathodic ECL behavior of cationic FF self-assembled peptide nanovesicles (PNVs) in aqueous

system.[10] As is well-known, for the ECL emitter, not only cathodic but also anodic ECL behaviors are of great importance, and their reaction mechanisms are completely different. However, to the best of our knowledge, there is no paper issued about the anodic ECL behavior of PNTs until now. Our motivation is to explore ECL behavior of various FF-based self-assembled nanostructures in aqueous system and expand their potential application in analytical field.

Herein, for the first time, we report the anodic ECL behavior of PNTs modified glassy carbon electrodes (GCEs) in the phosphate buffer solutions (PBS, pH 7.4) using tri-*n*-propylamine (TPrA) as the coreactant. Compared with the previous cathodic ECL of the PNVs,[10] the anodic ECL intensity of the PNTs had a remarkable increase. The anodic ECL reaction mechanism was explored. The preliminary application in the determination of metal ions was also demonstrated. The results suggested that PNTs could be a promising candidate for the construction of anodic ECL sensing platforms.

The PNTs were synthesized by self-assembly of FF monomers in aqueous solution according to the previous method (see ESI†).[4b] The corresponding characterization data are shown in Fig. 1B and Fig. S1 (ESI†). From the SEM image of the PNTs (Fig. 1B), it can be seen that a typical tubular structure with the diameters of 400 nm ~ 1 μm and the length of 80 ~ 300 μm. A typical TEM image (Fig. S1A, ESI†) of the PNTs further confirmed the hollow tubular structure. The XRD pattern of the PNTs displayed (Fig. S1B, ESI†) a series of sharp diffraction peaks, which is consistent with that of PNTs in the previous report.[11a] This indicated that the self-assembled PNTs had good crystallinity. The FTIR spectrum of the PNTs (Fig. S1C, ESI†) showed a strong peak at 1686 cm^{-1}, inferring that FF monomers were stacked in a *β*-turn arrangement with hydrogen boding.[11b] Furthermore, UV–Vis spectrum of the PNTs showed an identical spike-like behaviour (Fig. S1D, ESI†), suggesting the existence of identical nanosize regions of QDs in the structure of the PNTs.[4b] These results demonstrated that the prepared PNTs were similar to that previously reported,[4] which possessed good crystalline structure and QC properties.

For the study of the ECL behavior of the PNTs, the PNTs-modified GCE (PNTs/GCE) was fabricated. The freshly prepared suspension of the PNTs was dropped on the surface of clean GCEs and dried in room temperature for the following study. The detailed modified procedure was given in the supporting information. Fig. 2A shows the ECL curves of the bare (curve a) and PNTs/GCE (curve b) in 0.1 M PBS (pH 7.4) including 0.1 M NaCl and 20 mM TPrA by cycling the potential between 0.00 and 1.40 V vs. Ag/AgCl. Only a very weak ECL signal was observed on the bare GCE, which is similar to previously reported those at the other bare Au, Pt electrode or GCE in TPrA solution without luminescent species.[12] However, a quite intense ECL emission was obtained on the PNTs/GCE after 1.10 V. The results indicated that the strong ECL emission mainly originated from the PNTs. Furthermore, when the same concentration of FF monomer was modified on the surface of the GCE, the FF/GCE exhibited very low ECL response (Fig. S2 in the ESI†), which was similar to that of the bare GCE. This further suggested that the self-assembled structure of the PNTs might be key to the generation of the intense ECL response. This is reasonable that FF as monomer molecules did not show any special properties. Only when FF self-assembled into the PNTs, the PNTs exhibited exceptional electronic and photonic properties, which make them

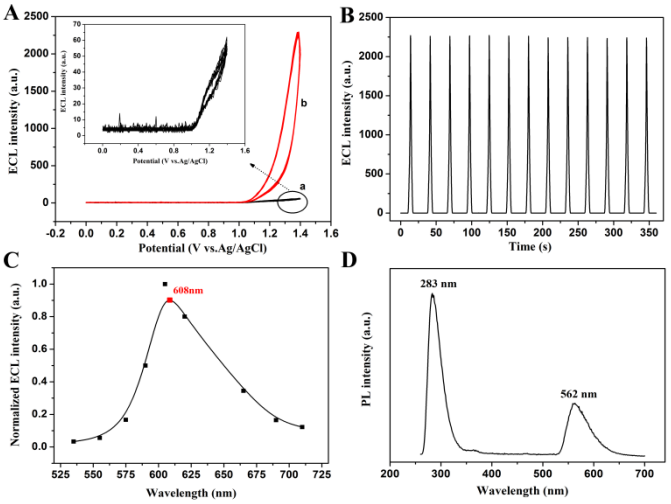

Fig. 2 (A) ECL potential curves of a bare GCE (a) and the PNTs/GCE (b) in 0.1 M PBS (pH 7.4) containing 0.1 M NaCl and 20 mM TPrA. The inset displays the enlarged view of curve a. (B) Time-dependent ECL signals of the PNTs/GCE. (C) ECL spectrum of the PNTs/GCE. (D) PL spectrum of the PNTs solid.

potential as illuminant body.[6] In addition, the ECL signal of the PNTs/GCE remained at an almost constant value during consecutive cyclic potential scanning (Fig. 2B), inferring the PNTs/GCE is potential as an ECL sensor.

The ECL spectra of the PNTs were also measured by employing a series of optical filters, and a distinguished ECL spectrum peak at approximately 608 nm was observed (Fig. 2C). Fig. 2D shows the PL spectrum of the PNTs solid under excitation at 257 nm. Two peaks located at about 283 and at 562 nm respectively were observed. The former is characterization of the phenylalanine residue[11c] and the latter is attributed to the assembled nanostructures.[4a] Compared with the PL emission spectrum peak of the PNTs at 562 nm, there was a significant spectral red shift between their ECL and PL. In the previous studies, there are also few materials such as silicon NCs[8a] and carbon NCs[8b] whose PL spectra did not agreed well with ECL spectra. The difference could be attributed to that these emitters depended more sensitively on surface chemistry and the presence of rich surface states or surface traps.[8a] Considering a single PNT is composed of millions of biological quantum dots, this integrated structure may lead to that the the PNTs are more sensitive to surface chemistry or have rich surface traps due to the presence of some contact interfaces between quantum dots. This probably resulted in that the ECL spectrum peak of the PNT occurred at different wavelength to its PL spectrum peak.

Furthermore, the anodic ECL spectrum peak (608 nm) of the PNTs/GCE was slightly different with cathodic that (627 nm) of the PNVs/GCE[10] by using the same measured method. In the previously reported ECL behavior of the graphite-like carbon nitride (g-C_3N_4),[13] its anodic ECL emission spectrum matched well with that of its cathodic ECL. Thus the present difference of the ECL spectra between the PNTs and PNVs may be related to the difference of obtained self-assembled nanostructures (one is tubes and the other is vesicle). Certainly, it is not absolutely excluded to the ECL measured error from the coarse wavelength interval of the band-pass filters. The detailed measurement is underway. If the ECL emission

View Article Online
DOI: 10.1039/C5CC05229G
COMMUNICATION

spectra from various FF and its derives self-assembled nanostructures are tunable, it should be very attractive for the diverse bioanalytical applications.

In order to explore the anodic ECL mechanism of the PNTs, the effect of the coreactant on the ECL behavior of the PNTs/GCE was further investigated. When TPrA was absent in reaction solutions, no obvious signal was observed on the PNTs/GCE (Fig. S3, ESI†). Compared with the strong ECL signal in the presence of TPrA (curve b in Fig. 2A), it indicated that TPrA played an crucial role in the ECL process as a coreactant. The anodic ECL pathways of semiconductor QDs in the presence of TPrA as the coreactant have been widely reported. According to the previous studies,[14] the possible anodic ECL mechanism of the PNTs/GCE was proposed as follows:

$$PNT - e^- \rightarrow PNT^{\bullet+} \quad (1)$$

$$TPrA - e^- \rightarrow TPrA^{\bullet+} \quad (2)$$

$$TPrA^{\bullet+} \rightarrow TPrA^{\bullet} + H^+ \quad (3)$$

$$PNT^{\bullet+} + TPrA^{\bullet} \rightarrow PNT^{*} + \text{TPrA fragments} \quad (4)$$

$$PNT^{*} \rightarrow PNT + h\nu \quad (5)$$

The positively charged PNT (i.e., $PNT^{\bullet+}$) may be produced from the electro-oxidation of PNT by a potential sweep to a sufficiently positive potential, as shown in eq 1. Coreactant TPrA used in the present work could be electro-oxidized to a cation ($TPrA^{\bullet+}$) (Fig. S4a, ESI†), as shown in eq 2, and then, $TPrA^{\bullet+}$ would subsequently decompose to produce a radical ($TPrA^{\bullet}$), as shown in eq 3, which can react with the oxidized form of PNT to produce the excited state PNT (PNT^{*}) via electron transfer (eq 4). Finally, an intense emission is obtained when PNT* decays back to the ground state PNT (eq 5). It is also noted that the oxidation peak of the PNTs could not be observed in the potential window (Fig. S4b, ESI†). The similar phenomenon has been observed in anodic ECL systems of rubrene nanoparticles[8d] and g-C_3N_4.[13b]

The effect of the size of the obtained PNTs on the ECL behavior was also investigated. When the tube diameter and length of the PNTs were varied by adjusting self-assembled conditions, the onset potential of the corresponding ECL did not altered and only ECL intensity changed (not shown). Furthermore, the relationship between the change of ECL intensity and the size of the PNTs was not distinctly regular. However, it was notable that the assembled perfect degree of the PNTs was closely related to the ECL intensity. When the tubes had some fracture or their integrity was destroyed, the obtained ECL emission intensity obviously decreased (Fig. S5, ESI†). The reason is possibly attributed to that the ECL emission of the PNTs generated from the crystalline structure. When the crystallization of the self-assembled PNTs is better, the produced ECL is stronger. The further studies are in progress.

A series of experimental parameters, including the volumes of PNTs dropped on the GCE, coreactant concentration, solution pH and scan rate, are investigated to acquire the optimal ECL performance, as depicted in Fig. S6 (ESI†). Under the optimized conditions, the ECL intensity of the PNTs/GCE in 0.10 M PBS (pH 7.4) containing 20 mM TPrA and the bare GCE in a standard solution of 0.10 M PBS (pH 7.4) containing 1.0 mM $Ru(bpy)_3^{2+}$ and 20 mM TPrA are roughly compared to estimate the relative ECL efficiency (Fig. S7, ESI†). The integrated ECL intensity of the PNTs is about 0.028 times of that of the standard solution. The emission efficiency of the anodic ECL of the PNTs is still lower.

Other several coreactants were also used for ECL system of the PNTs. The results were shown in Fig. S8 (ESI†). The oxalate ($C_2O_4^{2-}$) and sulfite (SO_3^{2-}) as the coreactant respectively, the PNTs/GCE showed the very weak ECL responses. Meanwhile, the amine-related systems overall exhibited higher ECL intensity. The highest ECL intensity was generated from the PNTs/TPrA system, which is possibly attributed to that $TPrA^{\bullet}$ has stronger oxidation ability.

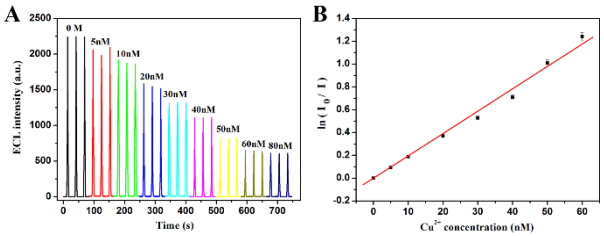

Fig. 3 (A) ECL profiles of the PNTs/GCE in the presence of different Cu^{2+} concentrations. (B) Linear calibration plot for Cu^{2+} detection.

To evaluate the possibility of the sensing application based on the ECL signal of the PNTs/GCE, metal ion Cu^{2+} was chosen as an analyst. Cu^{2+} plays a certain role in vital movements and some diseases such as Alzheimer's disease. Furthermore, Cu^{2+} is a significant pollutant. In previous study, it is reported that the ECL emission based on other semiconductors could be quenched statically by Cu^{2+}.[15] In this work, it is found that the ECL intensity of the PNTs/GCE was effectively quenched by trace amounts of Cu^{2+}, demonstrating its potential for Cu^{2+} determination.

Fig. 3A presents the effect of various concentrations of Cu^{2+} on the ECL intensity of the PNTs/GCE. Obviously, the ECL intensity decreased with the increase in Cu^{2+} concentration. Cu^{2+} could validly quench the ECL of the PNTs/GCE. Furthermore, in the absence of PNTs on the electrode or TPrA in the solution, no distinguishable change of the ECL signal was observed after nM Cu^{2+} was added into the solution. The Poisson statistics static quenching model[16] was employed to linearly relate the decrease in ECL intensity and concentration of Cu^{2+} by plotting ln (I_0/I) against the concentration of Cu^{2+} as shown in Fig. 3B, where I_0 and I are the ECL intensities in the absence and presence of Cu^{2+}, respectively. The curve had a linear range from 5 to 60 nM with a detection limit of 1.0 nM at a signal/noise ratio of 3, which is lower than or comparable with other Cu^{2+} sensors based on the ECL of CdTe QDs.[15] The main superiority of the proposed ECL sensor is that the ingredient is biocompatible and the synthesis of the PNTs is simple.

The selectivity of the present ECL sensor was also examined. The PNTs/GCEs were exposed to interfering metal ions (60 nM) in 0.10 M PBS (pH 7.4) containing 20 mM TPrA. Fig. S9 (ESI†) reveals that it had a good selectivity for Cu^{2+} over the potential interfering agents such as K^+, Mg^{2+}, Ca^{2+}, Zn^{2+}, Fe^{2+}, Pb^{2+}. The good selectivity may be attributed to higher affinity of Cu^{2+} to β-amyloid proteins[17] while FF was key component in the Alzheimer's β-amyloid.[2] In addition, the PNTs/GCE showed a good reproducibility with a relative standard deviation (RSD) of 3.0% for the detection of 40 nM Cu^{2+} under ten cycles of continuous potential scans. Five PNTs/GCEs prepared under the same condition exhibited an acceptable reproducibility with a RSD of 5.4% for the detection of 60 nM Cu^{2+}.

The present PNTs-based ECL sensor was also used to detect the

concentration of Cu^{2+} in river sample. The result showed a copper content of 50.9 ± 1.3 nM (n = 3) in river water, which agreed with the value of 48.8 nM obtained from inductively coupled plasma-atomic emission spectroscopic method. The result indicated that this method had acceptable selectivity and accuracy.

Conclusions

In summary, the intense anodic ECL emission was firstly obtained from the one-dimension PNTs modified electrode in PBS solutions containing TPrA as the coreactant. The possible ECL mechanism was proposed. The analytical application for the Cu^{2+} was also demonstrated based on the quenched ECL signal of the PNTs/GCE. Although the ECL efficiency of the PNTs in the present work is still lower and the potential of ECL emission is high, it may be further improved by changing the synthesized method[18a,b] and adjusting the reaction condition.[14,15a] The self-assembled PNTs derived from FF as a new ECL emitter are very promising in ECL bioanalytical applications because of their high biocompatibility, simple synthesis, tunable composition and structures, as well as the capability of molecular recognition. Finally, the study of the ECL behavior of these bionanostructure would be also beneficial to deeply understanding their novel properties.

This work was supported by the National Basic Research Program of China (2011CBA00508), the National Natural Science Foundation of China and Beijing Engineering Center for Hierarchical Catalysts.

Notes and references

[a]State Key Laboratory of Chemical Resource Engineering, Beijing University of Chemical Technology, Beijing 100029, P. R. China. E-mail: chenxu@mail.buct.edu.cn

† Electronic Supplementary Information (ESI) available: Characterization of prepared PNTs, ECL potential curves of the FF/GCE and PNTs/GCE in the absence of TPrA, cyclic voltammograms of the PNTs/GCE in the presence and absence of TPrA, effect of various conditions on the ECL response, ECL efficiency relative to $Ru(bpy)_3^{2+}$, ECL responses in the presence of different kinds of coreactants and selectivity of the present ECL sensor. See DOI: 10.1039/b000000x/

1 (a) A. Lakshmanan, S. Zhang and C. A. E. Hauser, *Trends Biotechnol*., 2012, **30**, 155–165; (b) Y. Cui, S. N. Kim, R. R. Naik and M. C. Mcalpine, *Accounts Chem. Res.*, 2012, **45**, 696–704; (c) S. Fleming and R. V. Ulijn, *Chem. Soc. Rev*., 2014, **43**, 8150–8177.

2 M. Reches and E. Gazit, *Science*, 2003, **300**, 625–627.

3 (a) X. Yan, P. Zhu and J. Li, *Chem. Soc. Rev*., 2010, **39**, 1877–1890; (b) L. Adler-Abramovich and E. Gazit, *Chem. Soc. Rev*., 2014, **43**, 6881–6893.

4 (a) N. Amdursky, M. Molotskii, D. Aronov, L. Adler-Abramovich, E. Gazit and G. Rosenman, *Nano Lett.*, 2009, **9**, 3111–3115; (b) N. Amdursky, M. Molotskii, E. Gazit and G. Rosenman, *J. Am. Chem. Soc*., 2010, **132**, 15632–15636.

5 (a) N. Amdursky, M. Molotskii, E. Gazit and G. Rosenman, *Appl. Phys. Lett.*, 2009, **94**, 261907; (b) N. Amdursky, E. Gazit and G. Rosenman, *Adv. Mater*., 2010, **22**, 2311–2315.

6 C. A. E. Hauser and S. Zhang, *Nature*, 2010, **468**, 516–517.

7 (a) W. Miao, *Chem. Rev.*, 2008, **108**, 2506–2553; (b) L. Hu, and G. Xu, *Chem. Soc. Rev*., 2010, **39**, 3275–3304.

8 (a) Z. Ding, B. M. Quinn, S. K. Haram, L. E. Pell, B. A. Korgel and A. J. Bard, *Science*, 2002, **296**, 1293–1297; (b) L. Zheng, Y. Chi, Y. Dong, J. Lin and B. Wang, *J. Am. Chem. Soc.*, 2009, **131**, 4564–4565; (c) Y. Fang, J. Song, J. Li, Y. Wang, H. Yang, J. Sun and G. Chen, *Chem. Commun.*, 2011, **47**, 2369–2371; (d) K. M. Omer and A. J. Bard, *J. Phys. Chem. C*, 2009, **113**, 11575–11578; (e) M. Hesari, J. Lu, S. Wang and Z. Ding, *Chem. Commun*., 2015, **51**, 1081–1084.

9 (a) J. Li, S. Guo and E. Wang, *RSC Adv.*, 2012, **2**, 3579–3586; (b) S. Deng and H. Ju, *Analyst*, 2013, **138**, 43–61; (c) Z. Liu, W. Qi and G. Xu, *Chem. Soc. Rev*., 2015, **44**, 3117–3142.

10 C. Huang, X. Chen, Y. Lu, H. Yang and W. Yang, *Biosens. Bioelectron*., 2015, **63**, 478–482.

11 (a) C. H. Görbitz, *Chem. Eur. J.*, 2001, **7**, 5153–5159; (b) X. Yan, Y. Cui, Q. He, K. Wang and J. Li, *Chem. Mater.*, 2008, **20**, 1522–1526; (c) E. Mihalyi, *J. Chem. Eng. Data*, 1968, **13**, 179–182.

12 Y. Zu and A. J. Bard, *Anal. Chem*., 2000, **72**, 3223–3232.

13 (a) C. Cheng, Y. Huang, X. Tian, B. Zheng, Y. Li, H. Yuan, D. Xiao. S. Xie and M. M. F. Choi, *Anal. Chem*., 2012, **84**, 4754−4759; (b) C. Cheng, Y. Huang, J. Wang, B. Zheng, H. Yuan and D. Xiao, *Anal. Chem.*, 2013, **85**, 2601–2605.

14 (a) L. Z, X. Zou, E. Ying and S. Dong, *J. Phys. Chem. C*, 2008, **112**, 4451–4454; (b) H. Jiang and X. Wang, *Electrochem. Commun*., 2009, **11**, 1207–1210.

15 (a) L. Zhang, L. Shang and S. Dong, *Electrochem. Commun*., 2008, **10**, 1452–1454; (b) Y. Mei, H. Wang, Y. Li, Z. Pan and W. Jia, *Electroanal*., 2010, **22**, 155–160.

16 A. V. Isarov and J. Chrysochoos, *Langmuir*, 1997, **13**, 3142–3149.

17 G. Arena, G. Pappalardo, I. Sovago and E. Rizzarelli, *Coordin. Chem. Rev*., 2012, **256**, 3–12.

18 (a) J. S. Lee, I. Yoon, J. Kim, H. Ihee, B. Kim and C. B. Park, *Angew. Chem. Int. Ed*., 2011, **50**, 1164–1167; (b) L. Adler-Abramovich, D. Aronov, P. Beker, M. Yevnin, S. Stempler, L. Buzhansky, G. Rosenmen and E. Gazit, *Nat. Nanotechnol.*, 2009, **4**, 849–854.